Mon. Not. R. Astron. Soc. **000**, 000–000 (0000) Printed 16 July 2015 (MN LATEX style file v2.2)

The effect of clumpy outflows and disc anisotropy on quasar unification scenarios

J. H. Matthews[1⋆], C. Knigge[1], N. Higginbottom[1], K. S. Long[2], S. A. Sim[3], and S. W. Mangham[1]

[1] *School of Physics and Astronomy, University of Southampton, Highfield, Southampton, SO17 1BJ, United Kingdom*
[2] *Space Telescope Science Institute, 3700 San Martin Drive, Baltimore, MD, 21218*
[3] *School of Mathematics and Physics, Queens University Belfast, University Road, Belfast, BT7 1NN, Northern Ireland, UK*

16 July 2015

ABSTRACT

Various unification schemes for quasars and luminous active galactic nuclei (AGN) have proposed that the broad emission line region is roughly cospatial with broad absorption line (BAL) gas and much of the phenomenology of luminous AGN can be explained by a simple geometrical picture involving an accretion disc and associated outflow. Here, we test this paradigm by utilising our state-of-the-art radiative transfer code to produce synthetic spectra from simple biconical disc wind models. In particular, we expand on our previous work in which a benchmark model for BAL quasars was produced. We find that a simple treatment of clumping ('microclumping') allows for a more realistic X-ray luminosity in the model by lowering the ionization parameter. We examine the X-ray properties of this new model and find good agreement with existing X-ray samples of AGN and QSOs. We find that clumping enhances the H recombination and collisionally excited resonance lines, causing strong line emission (EW=?) to emerge at the low inclination angles, which represent quasars within this unification scenario. However, we are unable to produce line emission with comparable equivalent widths to existing quasar composites, due to a fundamental constraint arising from the anisotropy of emission from a classical thin disc. We briefly explore the effect of relativistic beaming, gravitational redshift and light bending on the angular distribution of disc continuum emission. We find that these general relativistic effects do cause the disc to emit more isotropically, but this is not yet sufficient to produce a self-consistent model. We discuss a number of potential solutions. Overall, our work suggests that geometric unification involving an accretion disc wind is a promising scenario, but our results pose a number of difficult challenges to such a model.

1 INTRODUCTION

The spectral energy distributions (SEDs) of quasars and luminous active galactic nuclei (AGN) typically exhibit a series of strong emission lines (e.g. Ly α, C IV, N V) with an underlying blue continuum - the so-called *'big blue bump'* (BBB). The BBB is normally attributed to emission from a geometrically thin, optically thick accretion disc surrounding the central black hole (REF), similar to that described by Shakura & Sunyaev (1973). In addition to the inflowing accreting material, outflows are ubiquitous in AGN and quasars (REFs). These outflows can take the form of highly collimated radio jets (Belloni 2010)(BETTER REF), or mass-loaded 'winds' emanating from the accretion disc. Approximately 20% of quasars exhibit broad absorption lines (BALs) in the ultraviolet, providing clear evidence for outflowing absorbing material (Weymann et al. 1991; Reichard et al. 2003; Knigge et al. 2008; Turner & Miller 2009; Allen et al. 2011). The simplest explanation for the incidence of BAL quasars (BALQSOs) is in terms of an accretion disc wind (ADW). Within this paradigm, the BALQSO fraction is associated with the covering factor of the outflow.

It is possible that the diverse phenemonology of luminous AGN and QSOs can be broadly explained by into a simple picture of geometric unification (e.g. Murray et al. 1995; Elvis 2000). In such a model, a biconical wind rises from the accretion disc, and the class of object is explained by the material intercepting the line of sight. Depending on viewing angle, an observer may then see a BALQSO, LoBAL-QSO or normal 'Type 1' quasar. Within this framework, the broad-line region (BLR) is normally assumed to correspond to the dense wind base. A disc wind may also have a profound effect on the structure and emergent continuum of the accretion disc itself. Mass-loss will alter the accretion rate and resultant temperature of the accretion disc, possibly explaining some of the features we typically see in luminous AGN (Laor & Davis 2014). Recent results from Capellupo et al. (2015) find that if one includes a combination of mass-loss, general relativity (GR) and Comptonisation then AGN SEDs can, in general, be fitted well with

accretion disc models. In general, mass-loss treatments appear to be critical if an α-disc model is to successfully fit AGN SEDs, particular in the UV region of the spectrum.

Despite the clear importance of ADWs in understanding AGN SEDs and accretion physics, much of the underlying outflow physics remains highly uncertain. Several possible driving mechanisms for ADWs have been proposed, including thermal pressure (REFs), magnetocentrifugal forces (Blandford & Payne 1982) and radiation pressure on spectral lines ('line-driving' Lucy & Solomon 1970; Murray et al. 1995). Of these, line-driving is possibly the most attractive, due to the strong absorption lines seen in BALQSOs and the X-ray spectra of AGN (REFs). The presence of line-locked features (Bowler et al. 2014) and the so-called 'ghost of Ly α' (Arav 1996) in the spectra of such objects also gives clearer evidence that line-driving is at least partially contributing to the acceleration of the wind. The efficiency of line-driving is crucially dependent on the ionization state of the outflowing plasma. Murray et al. (1995) proposed a potential solution: a region of 'hitchhiking gas' that could shield the wind from the central X-ray source. Hydrodynamic simulations of line-driven disc winds also found a shielding region was required to maintain the correct ionization state (Proga et al. 2000; Proga & Kallman 2004). However, Higginbottom et al. (2014) showed that including multiple scattering means the ionizing radiation field could still reach the previously shielded regions in those particular models.

An alternative solution is that the wind is clumped (REFs), possibly on multiple scale lengths. Local density enhancements could lower the ionization parameter of the plasma while still maintaining the same mass-loss rate and column density. An inhomogenous outflow has been proposed as a model for the BLR (REFs) Clumping is expected in outflows and BLRs.

In this paper, we attempt to test the disc wind paradigm using Monte Carlo radiative transfer and photoionization calculations. In section 2, we describe our code. In section 3, we briefly discuss some of the successes and failures of our previous benchmark model for BALQSOs (Higginbottom et al. 2013, hereafter H13) and outline the model, including a description of our clumping prescription. In section 4, we present the results from a clumped model which successfully reproduces the observed ionization state while maintaing realistic X-ray properties. In section 5 we discuss our results, focussing particular on the anisotropy of disc emission and GR effects, and finally, in section 6, we summarise our findings.

2 IONIZATION AND RADIATIVE TRANSFER

We use the MCRT code Python to carry out our radiative transfer and photoionization calculations in non-local thermodynamic equilibrium (non-LTE). The code is described extensively by a series of authors (LK02, S05, H13, M15). For that reason we only briefly describe the key elements of the global ionization calculation and other important aspects.

2.1 Line transfer

To treat line transfer, we adopt the same hybrid scheme described by M15, in which the energy flows through the system are described in terms of indivisible energy quanta interacting with either 'simple ions' or 'macro-atoms'. The macro-atom implementation is described in full by Lucy (2002, 2003). The scheme allows one to treat non-LTE line transfer without approximation for elements which are identified as full macro-atoms.

2.2 Ionization Scheme

Macro-atoms have their ion and level populations derived from MC rate estimators as described by M15. To calculate the ionization fractions of simple-ions the dilute-blackbody modified Saha approach (Mazzali & Lucy 1993) is no longer appropriate due to the presence of a power-law X-ray source. Instead, we model the SED in a cell using the technique described by H13.

We improve on this method by abandoning the modified Saha approach entirely, and instead computing the ionization state by explicitly solving the rate equations in between ions in non-LTE. Photoionization and recombination rates are calculated using MC estimators recorded during the photon propagation. Not only does this dispense with a number of small assumptions made in the modified Saha approach, it is also more numerically stable, and in principle allows the direct addition of extra physical processes such as Auger ionization, which would have to be approximated if using the previous technique.

2.3 Atomic Data

We use the same atomic data as described by LK02 and since updated by H13 and M15, with the addition of direct ionization data from Dere (YEAR). Photoionization cross-sections are from Topbase (REF) and Verner et al. (1996).

3 A CLUMPY BICONICAL DISK WIND MODEL FOR QUASARS

Our kinematic prescription for a biconical disc wind model follows Shlosman & Vitello (1993), and is described further by LK02, H13 and M15. A schematic is shown in figure 1, with key aspects marked. The general biconical geometry is similar to that invoked by Murray et al. (1995) and Elvis (2000) in order to explain the phenomenonology of quasars and BALQSOs.

3.1 A Benchmark Model for BALQSOs

Higginbottom et al. (2013) presented a benchmark model for (BAL)QSOs...introduce key parameters.

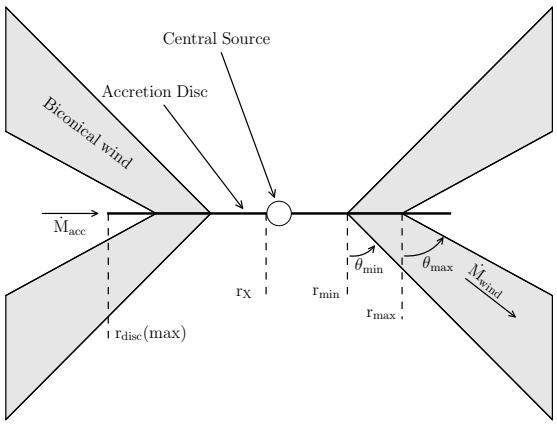

Figure 1. A cartoon showing the geometry and some key parameters of our biconical wind model.

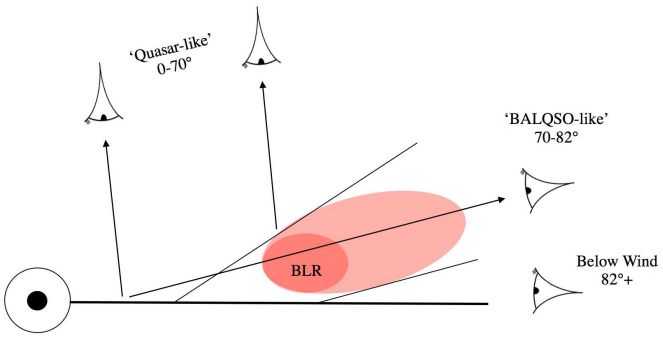

Figure 3. The classes of sightlines and the corresponding possible system types in the framework of our model. [FIGURE NEEDS IMPROVING]

3.1.1 Photon Sources

The accretion disc in our model is geometrically thin, but optically thick and this adopt a standard multi-temperature blackbody using a Shakura & Sunyaev (1973) temperature profile. The emergent SED is thus determined by the specified accretion rate ($\dot{m}$) and central BH mass (M_{BH}). The inner radius of the disc extends to the innermost stable circular orbit (ISCO) of the BH. We assume a Schwarzchild BH with an ISCO at 6 R_G. The X-ray source in our model is treated as an isotropic sphere at the ISCO, which emits photons according to a power law with index α_X. The normalisation of this power law is such that it produces the specified 2-10kev luminosity. In addition to the disc and X-ray source, the wind is able to reprocess radiation. However, new photon packets are not produced in the wind (as in LK02). Instead, this reprocessing is dealt with by enforcing strict radiative equilibrium via an indivisible energy packet constraint (see Lucy 2002, M15).

3.2 Potential for unification

What was wrong with H13 model - X-rays + BELs.

3.3 Clumping

Introduce microclumping.

4 RESULTS

Here we describe the results from our model.

4.1 Physical Conditions and Ionization State

The wind rises slowly from the disc at first, with clumped densities of $n_H \sim 10^{11}$ cm^{-3} close to the disc plane. The flow then accelerates over a scale length of $R_V = 10^{19}$ cm up to a terminal velocity of around 3 times the escape velocity ($\sim 10,000$ km s^{-1}). This gradual acceleration means that the wind exhibits a stratified ionization structure, with low ionization material in the base of the wind giving way to highly ionized plasma further out. By clumping the wind, we are able to produce the range of ionization states observed in Quasars and BALQSOs, while adopting a realistic $2-10$ keV X-ray luminosity of $L_X = 10^{43}$ ergs s^{-1}. Without clumping, this wind would be over-ionized to the extent that opacities in e.g., C IV would be entirely negligible (see H13).

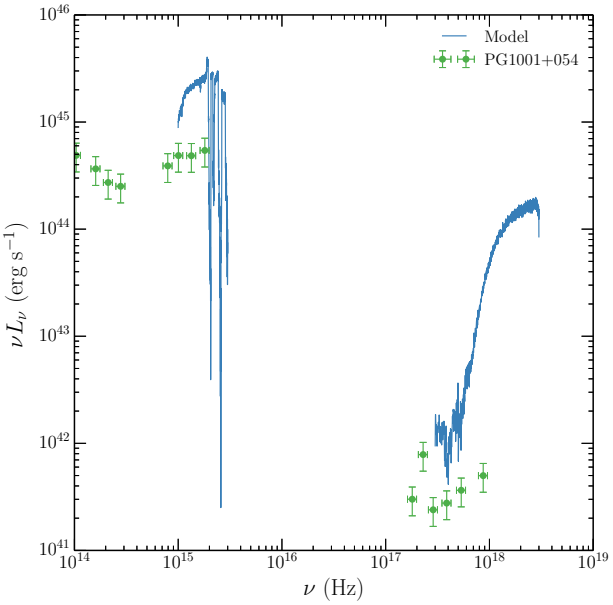

Figure 7. Broadband SEDs compared to IR and X-ray SEDs for selected BALQSOs from Grupe & Nousek (2015).

One commonly used measure of the ionization state is the ionization parameter, U, given by

$$U = \frac{4\pi}{n_H c} \int_{13.6\text{eV}}^{\infty} \frac{J_\nu d\nu}{h\nu}. \quad (1)$$

where n_H is the local number density of H, and ν denotes photon frequency. The ionization parameter represents the ratio of the number density of ionizing photons to the local H density. It is however, a poor measure of the ionization state of the resonance species such as C IV as it encodes no information about the shape of the SED. In this case

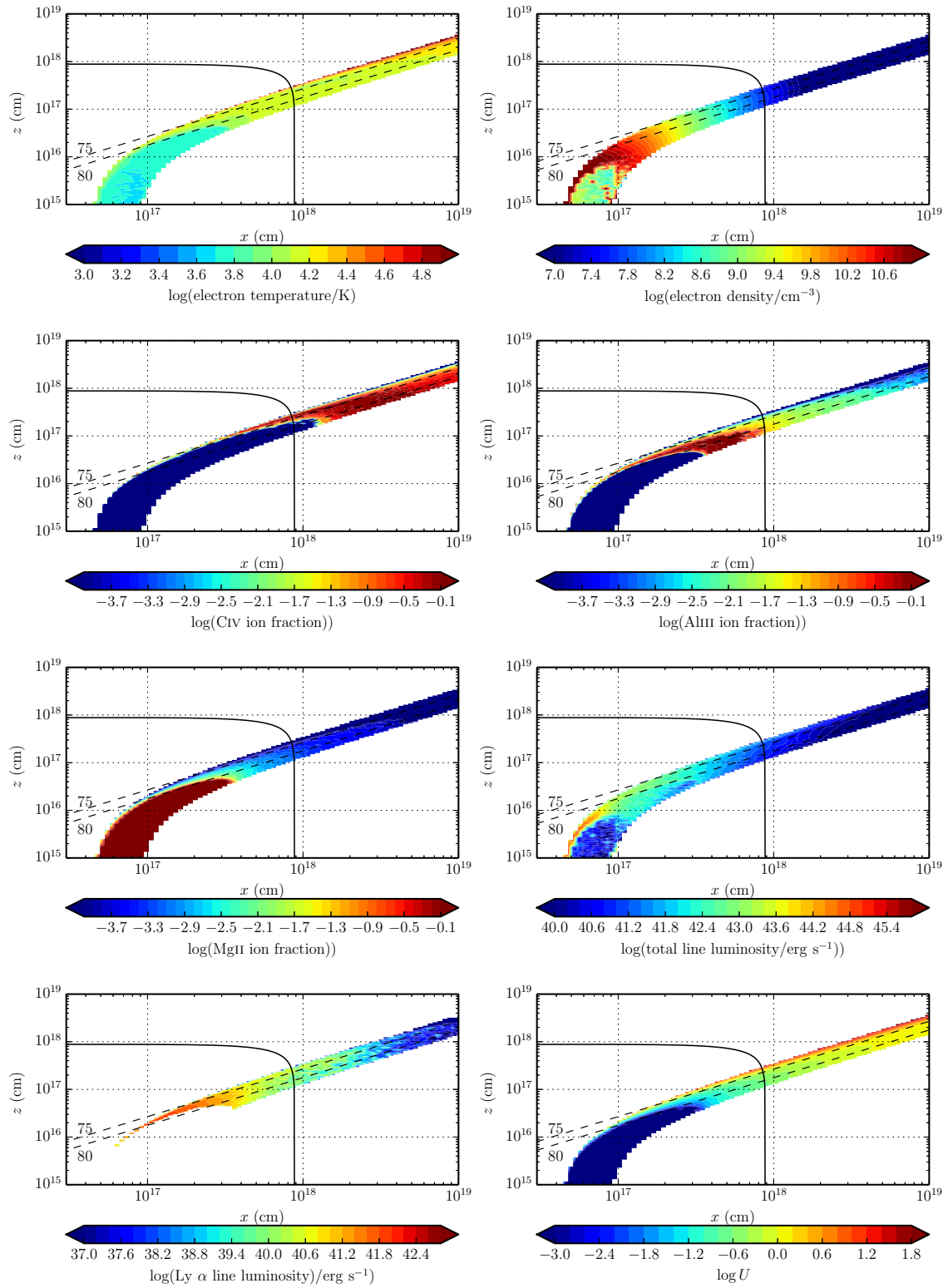

Figure 2. Physical properties of the outflow, shown by the coloured contours. The solid black line marks a sphere at 1000 R_G. The dotted lines show the 75° and 80° sightlines to the centre of the system, and illustrate that different sightlines intersect material of different ionization states.

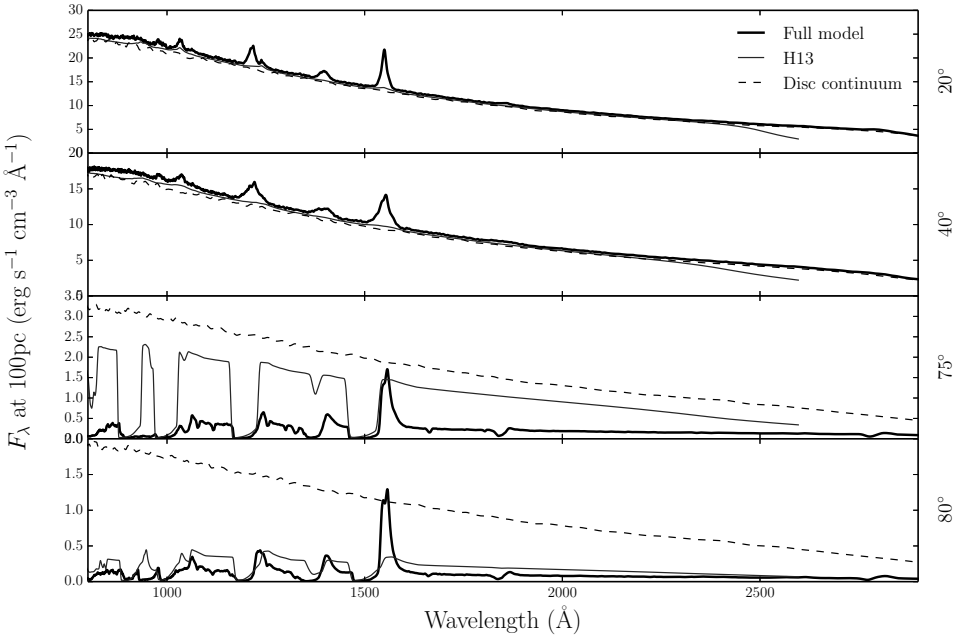

Figure 4. Synthetic spectra at four viewing angles in the clumpy model. Plot would look different probably, and may show composites, but this would be the main synthetic spectrum plot.

the X-ray photons are dominant in the photoionization of the UV resonance line ions. This explains why a factor of 100 increase in X-ray luminosity requires a clumping factor of 0.01, even though the value of U changes by roughly ?? compared to H13.

Clumping also causes the total line luminosity to increase dramatically, as recombination and collisional excitation are both proportional to n_e^2. This line emission typically emerges on the edge of the wind nearest the central source. The location of the line emitting regions is dependent on the ionization state, as well as the X-rays heating the plasma. The radii of these emitting regions is important, and can be compared to observations. Our C IV line emission region is located at about 1000 R_G ($\sim 10^{18}$ cm). This is in rough agreement with the reverberation mapping results of Kaspi (2000) for the $2.6 \times 10^9 M_\odot$ quasar S5 0836+71, and also compares favourably with microlensing measurements of the size of the C IV emission line region in the BALQSO H1413+117 (O'Dowd et al. 2015).

4.2 Synthetic Spectra

Present a spectrum of the UV and possible optical too.

4.3 X-ray Properties and Broadband SEDs

The bottom panel of figure 6 shows the emergent L_{2keV} monochromatic luminosity (L_ν) and α_{OX} plotted against L_ν at 2500Å for a number of different viewing angles in our model. α_{OX} is a spectral index from near UV to X-rays defined by

$$\alpha_{OX} = 0.3838 \log \left(\frac{L_\nu(2\ keV)}{L_\nu(2500\ \text{Å})} \right). \quad (2)$$

The properties are calculated from the synthetic spectra and thus include the effects of wind reprocessing and attenuation. In addition to model outputs, we also show the BALQSO sample of Saez et al. (2012) and luminous AGN and quasar samples from Steffen et al. (2006). For low inclination, 'quasar-like' viewing angles, we now show excellent agreement with AGN samples. The trend with inclination in our models is caused by a combination of disc foreshortening/limb-darkening (resulting in a lower L_{2500} for higher inclinations) and the fact that the disk is opaque and thus the X-ray source subtends a smaller solid angle at high inclinations (resulting in a lower L_{2keV} for higher inclinations).

Although the low inclination, 'BALQSO-like' viewing angles show moderate agreement with the data, it appears that our models tend to underpredict the emergent X-ray luminosity at although we are limited by poor statistics. It is possible that this is due to our wind being overly optically thick to electron scattering at angles which look through the wind. It could also be that the isotropic X-ray source assumption is incorrect and BALQSOs are *intrinsically* X-ray weak, as suggested by REFS. Nevertheless, our input X-ray spectrum now reproduces the X-ray properties of a luminous quasar.

Typically, BALQSOs show strong X-ray absorption with columns of $N_H \sim 10^{23}$ cm^{-2} (Green & Mathur 1996; Brandt et al. 2000; Mathur et al. 2000; Green et al. 2001; Grupe et al. 2003). This is often cited as evidence that the BAL outflow is shielded from the X-ray source, especially as sources with strong X-ray absorption tend to exhibit deep

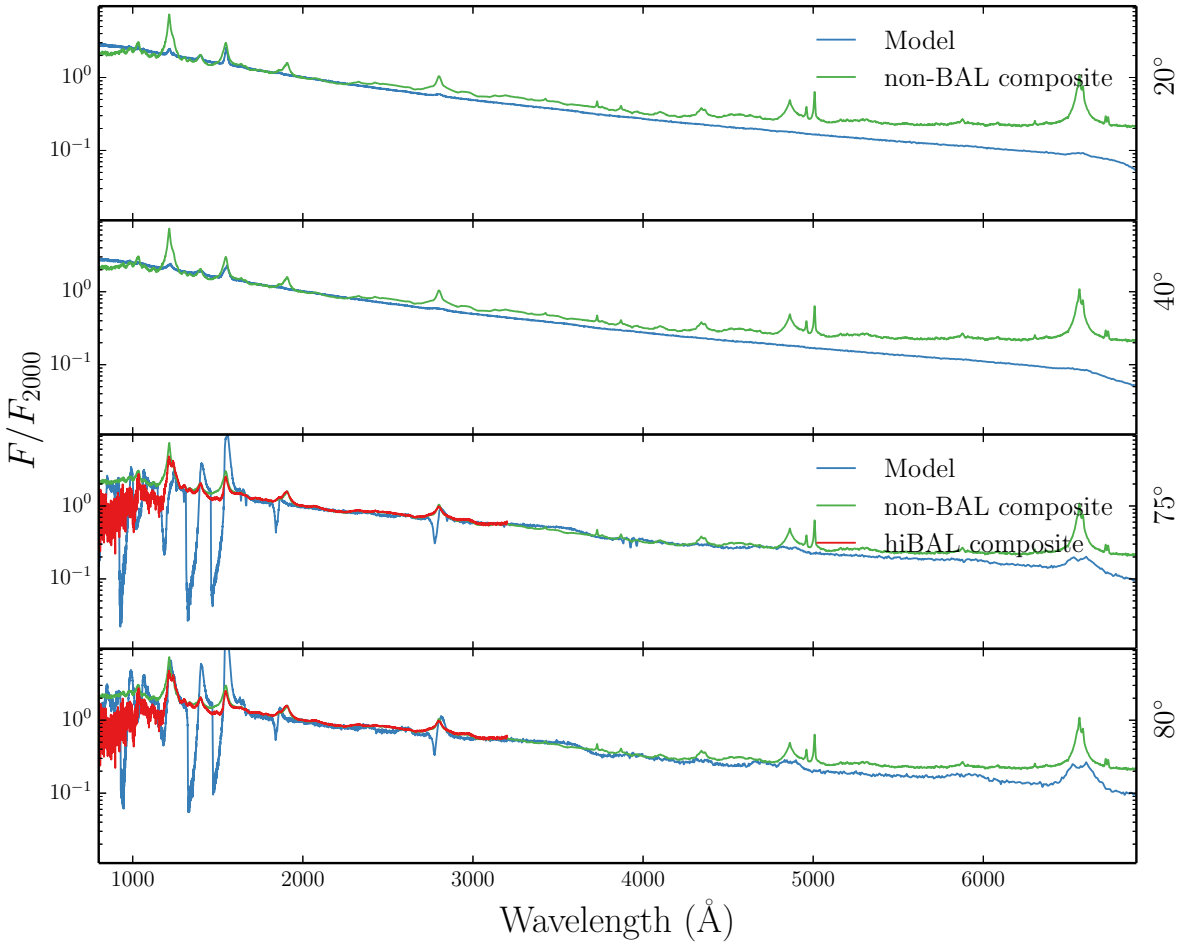

Figure 5. Figure designed to show optical spectrum and comparison to composite.

BAL troughs and high outflow velocities (REFs). Our results tend to imply that a clumpy BAL outflow itself can be responsible for the strong X-ray absorption, and possibly explains why mini-BALs have weaker X-ray absorption than BALQSOs (e.g. Brandt et al. 2000; Hamann et al. 2013).

We can also examine the emergent X-ray spectra from our model. Our code is not yet optimized for producing X-ray spectra, as we do not yet include all lines and levels of e.g. Fe or macro-atom treatments of higher order ions (cf. Sim et al. 2008, 2010). However, the bound-free opacity sources are complete, and comparisons of the shape of the heavily absorbed spectra can be useful. Figure 6 shows the broadband SED from the model, compared to a number of BALQSO spectra from Grupe & Nousek (2015) - note that lower mass and super-Eddington sources are excluded.

4.4 LoBALs and trends with inclination

At certain sightlines, our model now produces blue-shifted BALs in Al III and Mg II– the absorption lines seen in LoBALQSOs. Line profiles in velocity space for C IV, Al III and Mg II, are shown in figure 8 for a range of BALQSO viewing angles. We confirm the behaviour expected from a unification model such as Elvis (2000), in which ionization stratification explains the incidence of LoBALQSOs. In this framework, the lower ionization material is intercepted by a smaller family of sightlines. This is also the explanation here, as shown by figure **??**.

These line profiles also indicate a potential problem with our model. O'Dowd et al. (2015) find that the LoBAL profiles in H1413+117 have a higher velocity onset than the higher ionization BALs, suggesting that the wind becomes less ionized as radius increases. We find the opposite trend in velocity onsets. In addition, examination of figure **??** shows that ionization parameter decreases with radius, because the decrease in density wins over geometric dilution of the radiation field. While the O'Dowd et al. (2015) hypothesis comes from one object, it is clear that *at least some* BALQSOs must become less ionized at higher velocities, contrary to what one expects from our modelling.

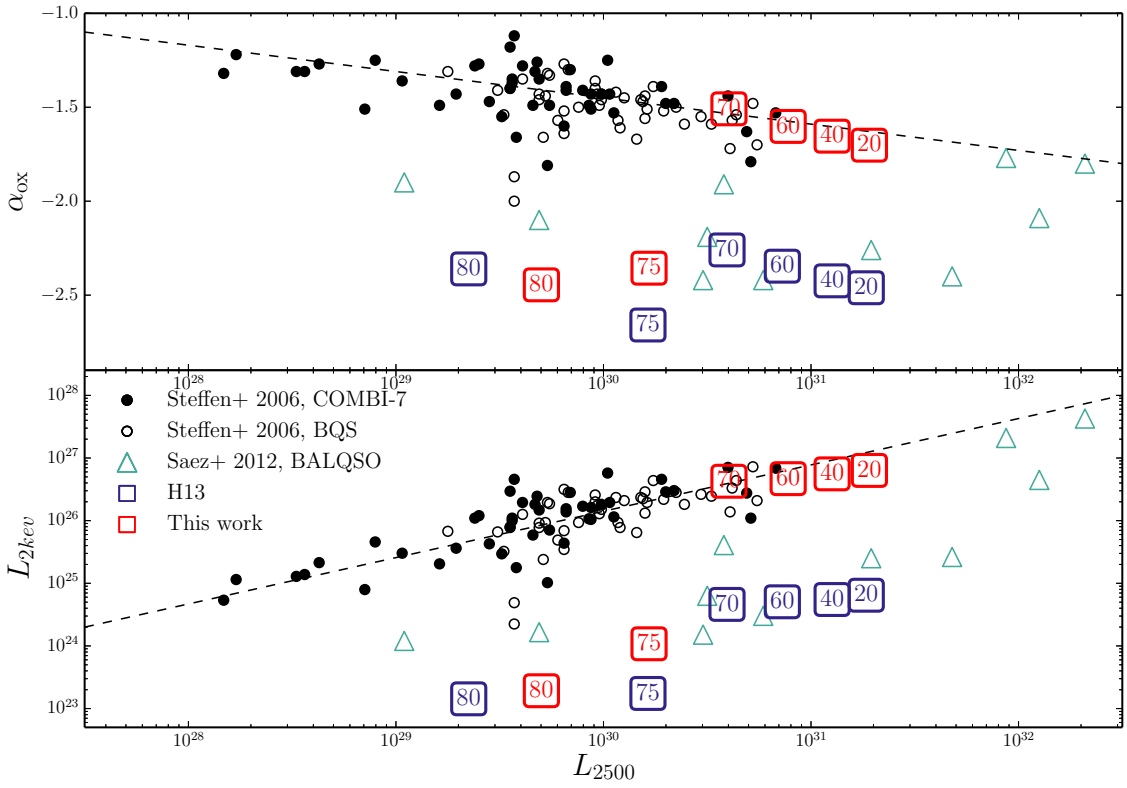

Figure 6. X-ray properties of the H13 and clumped model (text filled squares), plotted against monochromatic luminosity at 2500Å. Also plotted are the samples considered by Saez et al. 2012 on a similar plot; The COMBI-7 AGN sample (ref), the BQS sample (ref) and the Saez et al. (2012) sample of BALQSOs.

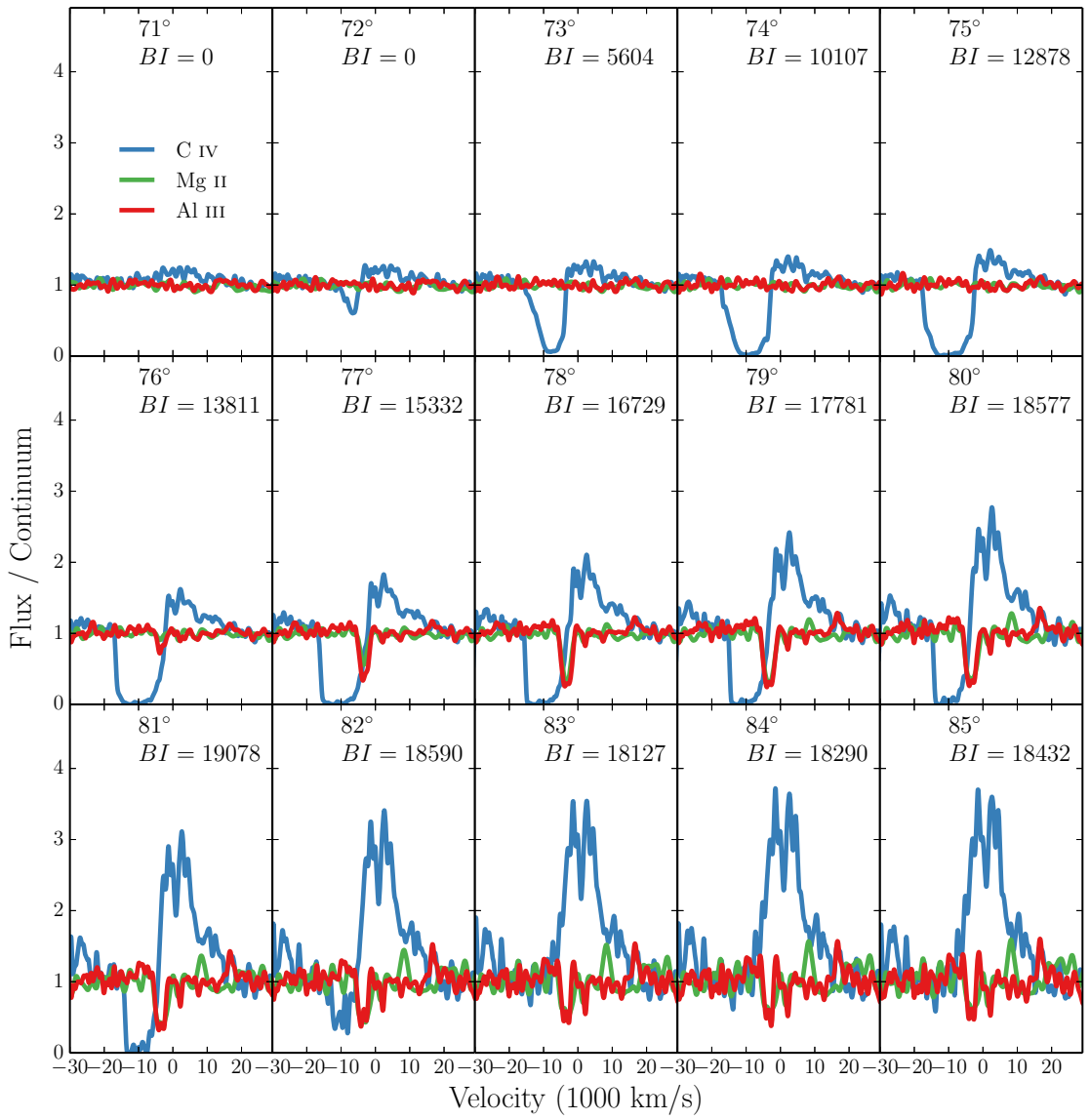

Figure 8. Carbon IV, Al III and Mg II line profiles with inclination for wind angles. Showing how the line profiles change and how LoBALs kick in at particularly high inclinations.

5 DISCUSSION

5.1 Anisotropy of disc emission

Discuss the importance of the angular distribution of the disc SED on line (limb-darkened, foreshortened, etc.)

5.2 General relativistic effects

Can GR effects offer a potential solution? (not quite!)

Figures 8 and 9: AGNSPEC F(2000) as a function of viewing angle compared to a BB disc. spectrum compared to composites with AGNSPEC correction.

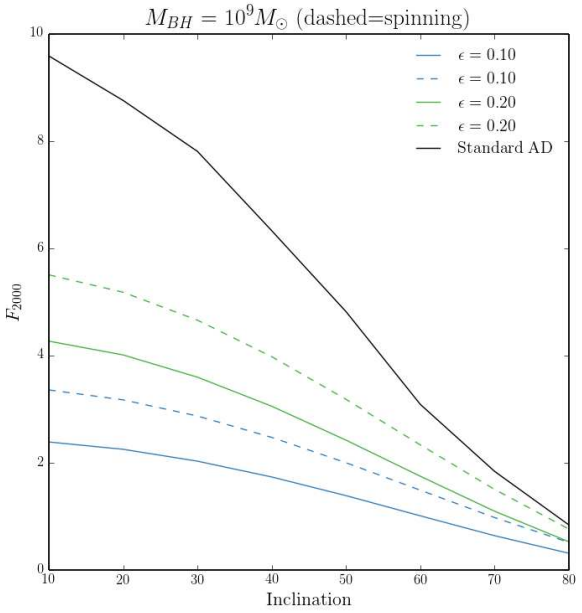

Figure 9. F_{2000} as a function of inclination from AGNSPEC models, compared to a classical AD. **This is a placeholder- it will show the effect of GR on the anisotropy of the disk for different wavelengths and eddington fractions, compared to limb darkened and foreshortened classical AD**.

a number of selection effects in building up the composites, and we should discuss these and the subtleties involved.

5.3 Wind reprocessing

How would wind reprocessing help?

5.4 The BALQSO fraction and wind covering factor

A brief comment, citing Goodrich / Krolik & Voit on the way in which anisotropy / attenuation affect the inferred BAL fraction. We also need to be aware that there will be

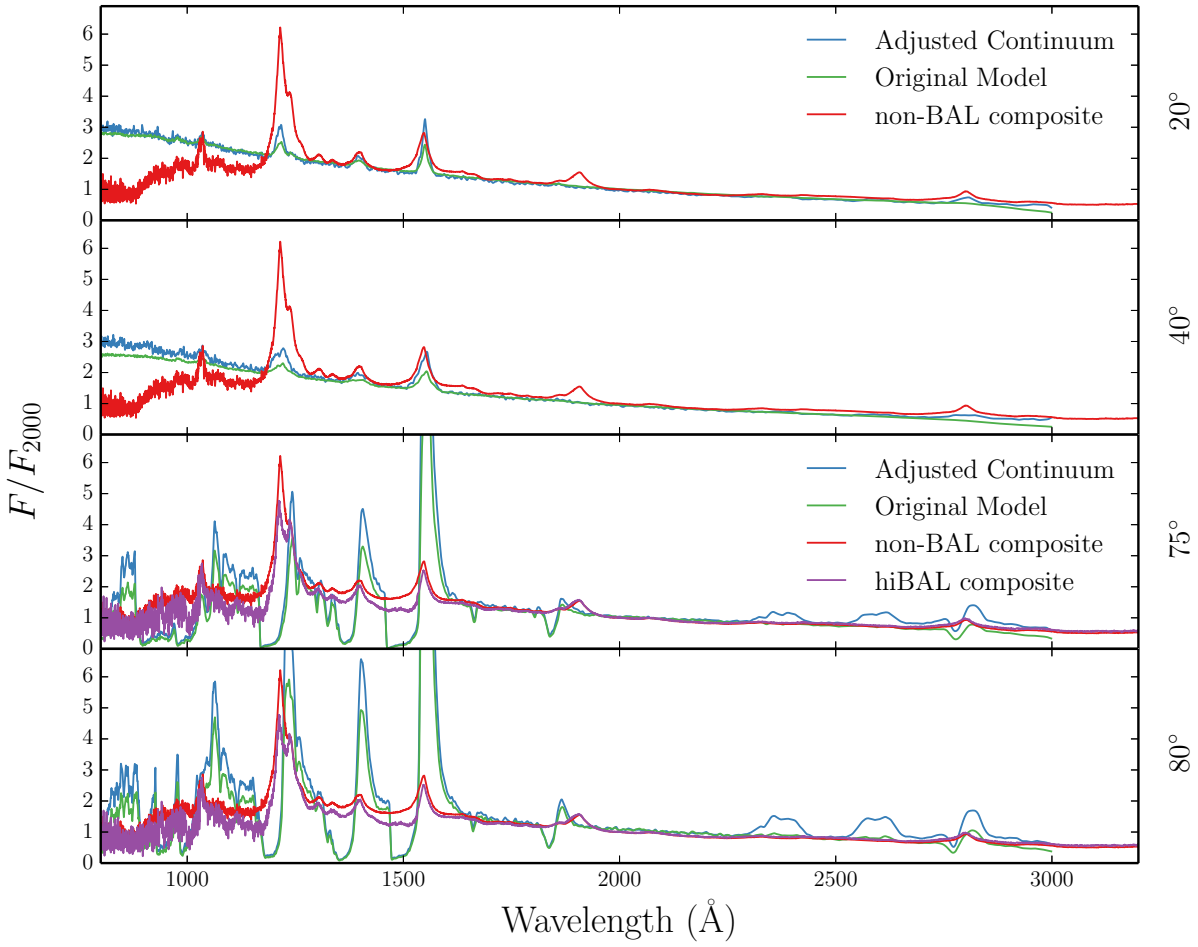

Figure 10. F_λ normalised to F_{2000}. **Again, this is a placeholder- but I'm thinking some kind of comparison to composite including the adjusted continuum, showing that we can't get it exactly right**.

6 SUMMARY

We have carried out MCRT simulations using a simple prescription for a biconical disc wind, with the aim of expanding on the work of H13 and assessing the viability of such a model for geometric unification of quasars. We find the following main points:

(i) We have introduced a first-order treatment of clumping in our model, and found that it can now maintain the required ionization state while agreeing well with the X-ray properties of AGN/QSOs.

(ii) We find that clumping also causes a significant increase in the strength of the emission lines produced by the model. This is true both of collisionally excited resonance lines (such as C IV, N V) and recombination lines (such as Ly α, H α and the Balmer series).

(iii) The line EWs in our models are not comparable to those in Quasar composite spectra. This is due to a fundamental constraint discussed in section ?. If the BLR emits fairly isotropically then for a foreshortened, limb-darkened classical thin accretion disc it is not possible to achieve line ratios at low inclinations that are comparable to those at high inclinations. This is a robust conclusion which is independent of the assumed BLR geometry.

(iv) We have examined the effect of GR on our disc SED, using the disc atmosphere and GR ray-tracing code AGNSPEC. While including GR effects does cause the disc SED to become significantly more isotropic, the effect is not large enough to produce uniform line to continuum ratios with viewing angle. We discuss other solutions to this problem in section ?; It is possible that a combination of GR and reprocessing by the wind could provide a solution, and a number of complicated selection effects may be at work in the building of the quasar composites.

Our work confirms a number of expected outcomes from such a model, and suggests that a simple geometry such as this can come close to explaining much of the phenomenology of quasars. Nevertheless, our conclusions pose a clear challenge to the current unification picture.

ACKNOWLEDGEMENTS

We would like to thank Omer Blaes, Ivan Hubeny, Shane Davis, Michael Crenshaw, Nahum Arav, Daniel Proga,

REFERENCES

Allen J. T., Hewett P. C., Maddox N., Richards G. T., Belokurov V., 2011, MNRAS 410, 860
Arav N., 1996, ApJ 465, 617
Belloni T. (ed.), 2010, The Jet Paradigm, Vol. 794 of *Lecture Notes in Physics, Berlin Springer Verlag*
Blandford R. D., Payne D. G., 1982, MNRAS 199, 883
Bowler R. A. A., Hewett P. C., Allen J. T., Ferland G. J., 2014, MNRAS 445, 359
Brandt W. N., Laor A., Wills B. J., 2000, ApJ 528, 637
Capellupo D. M., Netzer H., Lira P., Trakhtenbrot B., Mejía-Restrepo J., 2015, MNRAS 446, 3427
Elvis M., 2000, ApJ 545, 63
Green P. J., Aldcroft T. L., Mathur S., Wilkes B. J., Elvis M., 2001, ApJ 558, 109
Green P. J., Mathur S., 1996, ApJ 462, 637
Grupe D., Mathur S., Elvis M., 2003, AJ 126, 1159
Hamann F., Chartas G., McGraw S., Rodriguez Hidalgo P., Shields J., Capellupo D., Charlton J., Eracleous M., 2013, MNRAS 435, 133
Higginbottom N., Knigge C., Long K. S., Sim S. A., Matthews J. H., 2013, MNRAS 436, 1390
Higginbottom N., Proga D., Knigge C., Long K. S., Matthews J. H., Sim S. A., 2014, ApJ 789, 19
Knigge C., Scaringi S., Goad M. R., Cottis C. E., 2008, MNRAS 386, 1426
Laor A., Davis S. W., 2014, MNRAS 438, 3024
Lucy L. B., 2002, A&A 384, 725
Lucy L. B., 2003, A&A 403, 261
Lucy L. B., Solomon P. M., 1970, ApJ 159, 879
Mathur S., Green P. J., Arav N., Brotherton M., Crenshaw M., deKool M., Elvis M., Goodrich R. W., Hamann F., Hines D. C., Kashyap V., Korista K., Peterson B. M., Shields J. C., Shlosman I., van Breugel W., Voit M., 2000, ApJ Letters 533, L79
Mazzali P. A., Lucy L. B., 1993, A&A 279, 447
Murray N., Chiang J., Grossman S. A., Voit G. M., 1995, ApJ 451, 498
O'Dowd M. J., Bate N. F., Webster R. L., Labrie K., Rogers J., 2015, ArXiv e-prints
Proga D., Kallman T. R., 2004, ApJ 616, 688
Proga D., Stone J. M., Kallman T. R., 2000, ApJ 543, 686
Reichard T. A., Richards G. T., Hall P. B., Schneider D. P., Vanden Berk D. E., Fan X., York D. G., Knapp G. R., Brinkmann J., 2003, AJ 126, 2594
Shakura N. I., Sunyaev R. A., 1973, A&A 24, 337
Shlosman I., Vitello P., 1993, ApJ 409, 372
Turner T. J., Miller L., 2009, AAPR 17, 47
Verner D. A., Ferland G. J., Korista K. T., Yakovlev D. G., 1996, ApJ 465, 487
Weymann R. J., Morris S. L., Foltz C. B., Hewett P. C., 1991, ApJ 373, 23